International Journal of Pharmaceutics 421 (2011) 353–363

Contents lists available at SciVerse ScienceDirect

International Journal of Pharmaceutics

journal homepage: www.elsevier.com/locate/ijpharm

Pharmaceutical Nanotechnology

Drug solubilization by amino acid based polymeric nanoparticles: Characterization and biocompatibility studies

Pranabesh Dutta, Joykrishna Dey*

Department of Chemistry, Indian Institute of Technology, Kharagpur 721302, India

ARTICLE INFO

Article history:
Received 25 July 2011
Received in revised form
30 September 2011
Accepted 1 October 2011
Available online 6 October 2011

Keywords:
Hydrophobically modified polyelectrolytes
Nanoparticles
Griseofulvin
Solubilization
Fluorescence
Toxicity

ABSTRACT

Three novel amino acid based amphiphilic copolymers, poly(sodium *N* acryloyl-L-aminoacidate-*co*-dodecylacrylamide) (where aminoacidate = glycinate, leucinate, and phenylalaninate) were synthesized and characterized. These hydrophobically modified polyelectrolytes (HMPs) formed spheroidal nanoparticular aggregates above a critical aggregation concentration with average diameter 20–200 nm and overall negative charges as indicated by dynamic light scattering (DLS) and zeta-potential ($\zeta \approx -10.2$ to -25.2) measurements, respectively. The size and shape of the nanostructures was confirmed by transmission electron microscopic images. The micropolarity and microviscosity of the nanosize aggregates were investigated by fluorescence probe method using extrinsic probes like *N*-phenyl-1-naphthylamine, pyrene, and 1,6-diphenyl-1,3,5-hexatriene. The stability of the copolymer micelles was investigated as a function of pH and temperature using fluorescence and DLS techniques. Both fluorescence probe and DLS data suggest that the copolymer micelles are highly stable under physiological condition (pH 7.4, 37.4 °C). These HMP micelles were evaluated primarily as a drug delivery system. The ability of the copolymers to encapsulate hydrophobic drug was investigated using a poorly water-soluble antifungal drug, griseofulvin. Biocompability of the HMPs were examined by hemolytic and cytotoxicity assay. All three HMPs were non-hemolytic up to the tested concentration of about 1.0 g/L. In vitro biological assay indicated that these new copolymers were also less toxic against 3T3 mammalian cell line. The studies suggest that these newly conceived amino acid based biocompatible polymeric nanoparticles might have potential application as injectible drug delivery systems which can enhance the therapeutic index of poorly water-soluble clinically challenging drugs.

1. Introduction

Hydrophobically modified polyelectrolytes (HMPs) have recently attracted much attention as promising materials for use in biomedical and pharmaceutical applications (York et al., 2008; Otsuka et al., 2003; Kedar et al., 2010; Li et al., 2010; Chiu et al., 2010; Aumelas et al., 2007; Kim et al., 2010). HMPs undergo spontaneous self-association through hydrophobic interaction in water. Unlike block copolymers, many of these HMPs depending upon degree of hydrophobic substitution do not display any specific critical micelle concentration (*CMC*) values, rather form different type of micellar aggregates, such as unimer micelles, unicore multipolymer micelles, and polycore multipolymer micelles through hydrophobic interaction within a single polymer chain (intra-molecular association) or between different polymer chains (inter-molecular association) which are more tightly packed and less mobile in contrast to low-molecular-weight surfactant micelles (Morishima, 1994; Yamamoto et al., 1998; Noda and Morishima, 1999; Yamamoto and Morishima, 1999). Because of this remarkable property this class of copolymers finds potential uses in biomedical applications. Several natural hydrophilic molecules, such as dextran, chitosan, pulluan, etc. have recently been chemically modified with the same objectives (Durand et al., 2004; Delgado et al., 2001; Ravi Kumar et al., 2004; Kim et al., 2001; Sallustio et al., 2004; Hirakura et al., 2004).

Among numerous synthetic polymers that have received attention as promising biomaterials, the polymers containing amino acid units as one of the constituents are potentially useful in many different biomedical applications, such as tissue engineering scaffolds, and drug delivery matrices (Guo et al., 2007; Lee et al., 2007; Yu et al., 2007; Pilkington-Miksa et al., 2007; Brown et al., 2003). Amino acid based polymers generally possess good mammalian cell compatibility and yield benign hydrolysis products. As a result, a large fraction of amino acids were used to produce synthetic poly(amino acid)s to study their characteristic polymerization behavior, structures, and properties (Murata et al., 1996; Mori et al., 2005; Casolaro et al., 2004, 2006). Synthetically derived poly(amino acid)s have various unique properties that make them attractive

* Corresponding author. Tel.: +91 3222 283308; fax: +91 3222 255303.
E-mail address: joydey@chem.iitkgp.ernet.in (J. Dey).

0378-5173/$ – see front matter © 2011 Elsevier B.V. All rights reserved.
doi:10.1016/j.ijpharm.2011.10.011

candidates as polymeric biomaterial. These contain ionizable pendant groups which provide improved pH responsiveness at around their pK_a. L-Leucine and L-phenylalanine are two essential amino acids which have strong hydrophobic nature based on their isobutyl and phenyl group, respectively and play an important role in helix formation. Poly(L-leucine) has been examined as a biocompatible material such as artificial skin and fiber (Kuroyanagi et al., 1987, 1990). Because of the tyrosine precursor, poly(L-phenylalanine) on the other hand were explored as an anti-depressant and mood elevator (Sabelli, 1991).

Although the polymers composed of amino acids alone have been widely explored, it is often found that these have limited thermal stability and solubility which restricts their use in pharmaceutical applications. The issue of solubility can, however, be resolved by adding hydrophobic functionality to the amino acid based polymeric systems. The polymer with amino acid and a few mol% of hydrophobic group will create an amphiphilic structure which will enable them to form different types of self-assembled nanostructures in aqueous solution. Thus, analogous to low-molecular-weight surfactant micelles, these nano-aggregates will be able to encapsulate poorly water-soluble pharmaceutical compounds into the inner hydrophobic core. Though this strategy has a great potential from the pharmaceutical point of view, to the best of our knowledge, there is hardly any report in this direction using amino acid as a constituent. Towards the development of soluble amino acid based polymer for drug delivery applications, recently, we have reported for the first time, the synthesis, self-aggregation behavior, drug encapsulation and release properties of a new class of amino acid based water-soluble amphiphilic polymers, poly(sodium *N*-acryloyl-L-valinate-*co*-alkylacrylamide) that consist of sodium *N*-acryloyl-L-valinate and alkylacrylamide of different degrees of hydrophobic substitution and chain length (Dutta et al., 2009a). We observed that the copolymer poly(sodium *N*-acryloyl-L-valinate-*co*-dodecylacrylamide), SAVal-DA(0.16) with 16 mol% dodecyl side chain content has a stronger hydrophobic association with good environmental stability under physiological condition (pH 7.4, temperature = 37.4 °C). Along with high drug loading capacity for hydrophobic antifungal drug griseofulvin, GF (Chart 1) it showed sustained drug release properties over a period of more than 3 days (Dutta et al., 2009b). In addition, it exhibited excellent in vitro biocompatibilities which further opened up the possibility of this copolymer for future drug delivery applications (Dutta et al., 2011). Though the effect of hydrophobic group has a great influence on the self-assembly properties, drug solubilization, and release behavior, we expect that the behavior of the copolymers will also be influenced by the nature of the hydrophilic group and in turn will affect the morphology and stability of the aggregates formed by the HMPs in aqueous solution. Moreover, incorporation of L-leucine and L-phenylalanine as amino acid constituent will play an important role in macromolecular conformation and assist the copolymers to become more improved in terms of thermal stability and biocompatibility. Therefore, encouraged by our interesting preliminary results using SAVal-DA(0.16), we further synthesized three new amino acid based copolymers poly(sodium *N*-acryloyl-L-aminoacidate-*co*-dodecylacrylamide)s, SAGly-DA(0.16), SAPhe-DA(0.16), and SALeu-DA(0.16) with glycinate, L-phenylalaninate, and L-leucinate as hydrophilic head group, respectively, of fixed hydrophobe content (16 mol%) and studied their self-assembly behavior and biocompatibility properties. The self-assembly behavior, and environmental stability of these HMPs were compared with the previously reported copolymer, SAVal-DA(0.16) of identical hydrophobic substitution. Drug loading properties of the present copolymers were primarily investigated for the model drug GF under physiological condition. Biocompatibilities were examined in terms of hemolysis and MTT assay.

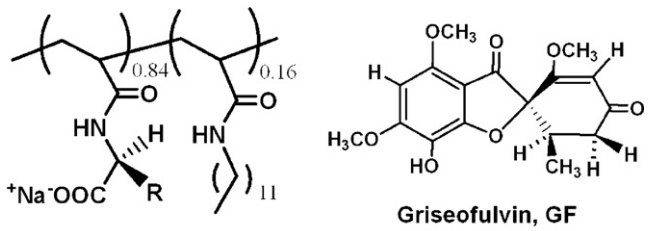

Griseofulvin, GF

SAGly-DA(0.16) x = 0.16, R = H

SALeu-DA(0.16) x = 0.16, R = $CH_2CH(CH_3)_2$

SAPhe-DA(0.16) x = 0.16, R = CH_2Ph

Chart 1. Chemical structure of copolymers and drug used in this report.

2. Experimental

2.1. Materials

Glycine, L-phenylalanine, and L-leucine were purchased from SRL (Mumbai, India) (SRL). Acryloyl chloride was obtained from MERK, Germany. Chloroform-d ($CDCl_3$), deuterium oxide (D_2O), dimethyl sulfoxide-d_6 (DMSO-d_6), 3-(4,5-dimethyl-2-thiazolyl)-2,5-diphenyl-2H-tetrazolium bromide (MTT) and griseofulvin (GF) were purchased from Sigma–Aldrich (St. Louis, MO, USA) and were used without further purification. 2,2′-Azobis(isobutyronitrile) (AIBN) was obtained from Sigma–Aldrich and were recrystallized from methanol. Dimethylformamide (DMF) was distilled over CaH_2 before use. The fluorescence probes pyrene, 1,6-diphenyl-1,3,5-hexatriene (DPH), *N*-phenyl-1-naphthylamine (NPN) were from Aldrich (Milwaukee, WI, USA) and were used after recrystallization from ethanol or acetone–ethanol mixture. Fluorescence emission and excitation spectra were used to check the purity of the probes. Milli-Q water (18.2 MΩ) obtained from Millipore water purification system was used for all the experiments.

The amino acid based copolymers were synthesized by means of free radical polymerization between the hydrophilic monomers sodium *N*-acryloyl-L-aminoacidates and hydrophobic monomer *N*-dodecylacrylamide following literature reported method (Dutta et al., 2009a; Kawata et al., 2007). The synthetic routes and the details of preparation of monomers and polymers are available under "Supplementary Materials". The polymerization was confirmed by the disappearance of the IR absorption and ^{1}H NMR chemical shift positions of the vinyl group. Further, broadening of the absorption peaks in the NMR spectrum indicated polymeric structure.

2.2. General characterization

Melting points of the synthesized compounds were determined with an Instind (Kolkata) melting point apparatus in open capillaries. The pH measurements were done with a digital pH meter Model pH 5652 (EC India Ltd., Kolkata) using a glass electrode. The UV–visible spectra were recorded on a Shimadzu (model 1601) spectrophotometer. The optical rotation was measured with P-1020 digital polarimeter (Jasco). Molecular weight and polydispersity index (PDI) of the copolymers were determined by gel permeation chromatography (GPC) with polystyrene as molecular weight standards (Spectra Physics Instruments equipped with a Shodex RI-101 refractometer detector and two 300 mm columns) using DMF (HPLC grade) as an eluent at a flow rate of 0.8 mL/min at 70 °C.

2.3. Viscosity measurements

Specific viscosity (η_{sp}) of aqueous polymer solutions were measured by use of a glass Ubbelohde viscometer (ASTM-D-446) with a flow time of 180 s for pure water immersed in water bath maintained at 30 °C. The density measurement was performed by use of portable digital density meter (Densito 30 PX, Mettler-Toledo, GmbH). All measurements were carried out at room temperature (~30 °C) unless otherwise mentioned. Flow-through times of copolymer solutions at various concentrations were determined at least five times for each concentration. Specific viscosities were determined by comparison with flow-through times of buffer solution.

2.4. Surface tension measurements

Surface tension (γ) was measured with a surface tensiometer (model 3S, GBX, France) at ~30 °C using the Du Nuöy ring detachment method. The platinum ring was regularly cleaned with ethanol–HCl solution and it was burnt in oxidizing flame by use of a Bunsen burner. Before each experiment the instrument was checked by measuring the surface tension of distilled water. Stock solutions of copolymers were made in buffered water. Aliquot of this solution was transferred to a beaker containing known volume of water. Magnetic stirring for 30 s followed by each addition of aliquot and allowed to stand for about 30 min at room temperature (~30 °C) to achieve equilibrium before surface tension was measured. For each concentration, three measurements for γ were performed and their mean was taken as the value of the equilibrium surface tension.

2.5. Steady-state fluorescence measurements

The steady-state fluorescence spectra of pyrene and NPN were measured with a SPEX Fluorolog-3 spectrofluorometer. The samples containing pyrene and NPN were excited at 335 nm and 340 nm, respectively and the emission intensity was recorded in the wavelength range 350–500 nm. Each spectrum was corrected for solvent fluorescence. Stock solutions of pyrene and NPN were prepared by adding the compound to buffer solution and magnetically stirred for 24 h. The excess compound was removed by centrifugation followed by filtration through Millipore syringe filter (0.22 μm) to obtain probe-saturated solution which was used for sample preparation. DPH was used as the fluorescence anisotropy probe. The concentration of DPH was adjusted to (2×10^{-7} M) by adding appropriate amount of ethanol stock solution. Steady-state fluorescence anisotropy (r) of DPH was measured on a PerkinElmer LS-55 spectrophotometer equipped with a thermostating cell holder and filter polarizer/analyzer assembly that used the L-format configuration. The excitation wavelength was set at 350 nm and the emission was monitored at 450 nm. A 430 nm cut-off filter was placed in the emission beam between emission monochromator and the analyzer to reduce the effect of scattered radiation. Each anisotropy measurement was repeated at least six times and an average value of r was recorded. The temperature of the samples was controlled using the water jacketed magnetically stirred cell holder in the spectrometer connected to Thermo Neslab RTE-7 circulating water bath that enables the temperature control within ±0.1 °C. Temperature dependent fluorescence measurements were performed in the range of 20–60 °C with an increment of 5 °C. Before every measurement, the solution was equilibrated at the desired temperature for at least 10 min.

Fluorescence lifetimes were determined from time-resolved intensity decays by the method of time-correlated single-photon counting using a pico-second diode laser at λ = 370 nm (IBH, UK, nanoLED-07) as the light source for excitation. The fluorescence decay kinetics of DPH was recorded at the emission wavelength of 450 nm. The decays were analyzed using IBH DAS-6 decay analysis software.

2.6. Dynamic light scattering

The dynamic light scattering (DLS) measurements were carried out using a home-built light scattering spectrophotometer equipped with a 100 mW He–Ne laser source (λ = 532 nm) at one arm of a goniometer, at varying scattering angles (θ = 40°, 60°, 80°, 90°, 100°, and 120°). The scattered beam was collected by a photo-multiplier tube (PMT) detector, mounted on other arm of the goniometer, and fed to a 256-channel digital correlator (7132 Malvern, UK) with 50 ns initial delay time. The temperature was set at 25 °C, unless changed to set other values. Prior to the measurements, each solution was cleaned by centrifuging at a speed of 5000 rpm for 15 min followed by filtration through a 0.45 μm filter paper (Millipore Millex syringe filter) and then loaded into an optical quality cylindrical quartz sample cell. The data acquisition was carried out for 2 min and each experiment was repeated at least twice. The apparent diffusion coefficients (D_{app}) were calculated by cumulant analysis (first order) of an autocorrelation function generated by the scattered light intensity fluctuations. The corresponding hydrodynamic radius (R_h) of the polymer aggregate was obtained using the Stokes–Einstein equation, $D = k_B T/(6\pi\eta R_h)$, where k_B is the Boltzmann constant and η is the solvent viscosity at temperature T.

2.7. Zeta potential measurements

The surface zeta potential of the copolymers were also measured using Zetasizer Nano ZS (Malvern Instrument Laboratory, Malvern, U.K.) optical system equipped with an He–Ne laser operated at 4 mW (λ_o = 632.8 nm) at 25 °C. The concentrations of the copolymers were kept at 1 g/L with either pH 5/7.4 (50 mM PBS). Three successive measurements were taken for each sample.

2.8. Transmission electron microscopy

High resolution transmission electron micrographs were obtained with a JEOL-JEM 2100 (Japan) electron microscope operating at an accelerating voltage of 200 kV at room temperature. A 5 μL volume of solution was placed on a 400 mesh size carbon-coated copper grid, allowed to stand for 1 min. The excess liquid was blotted with filter paper, air-dried. The specimen was kept in desiccators overnight for drying before measurement.

2.9. Solubilization studies

Solubilization studies were carried out following our previous report (Dutta et al., 2009b). Briefly, fine particles of GF were dissolved in 5 mL polymer solution of desired concentration (1 g/L) in screw-caped test tube. The solution containing the polymers and the drug was subsequently left under stirring for 5 days at 37 °C to ensure the solubilization equilibrium. The insoluble GF was removed by centrifugation at a speed of 4000 rpm for 10 min followed by careful filtration of the supernatant using Millipore Millex filter (0.45 μm pore diameter). An aliquot of these samples was diluted with methanol and absorbance value was measured by a UV–vis spectrophotometer at a wavelength of 292 nm using the previously recorded calibration curve. The copolymer solution at the same dilution was used as a blank. The same procedure was also applied to a solution of GF equilibrated with water to determine their water solubility and make necessary correction. Solubilization

capacities (S_{cp}) and encapsulation efficiency (E_{ef}) were calculated for 1 g/L copolymer solution according to the following equations:

$$S_{cp}(\text{mg/g}) = \frac{S^{G}_{poly} - S^{G}_{water}}{C_{poly} - CAC} \quad (1)$$

$$E_{ef} = \frac{\text{amount of drug encapsulated in polymer(mg)}}{\text{amount of drug added (mg)}} \times 100 \quad (2)$$

where S^{G}_{poly} is the solubility of drug in copolymer solution (mg/L), S^{G}_{water} is the solubility of drug in water (mg/L), C_{poly} is the concentration of the copolymer in g/L (1.0 g/L), and *CAC* is the critical aggregation concentration.

2.10. Biocompatibility studies

2.10.1. Hemolytic assay

Hemolytic assay was performed using the protocol reported by Katanasaka et al. (2008) with some modification. The copolymers were dissolved in sterile water to desired concentrations (0.1 and 1 g/L). Blood was obtained from 6-week-old BALB/c male mice and red blood cells (RBC) were collected by centrifugation (1500 rpm, 5 min, and 4 °C) of the blood. The collected RBC pellet was diluted in 20 mM HEPES buffered saline (pH 7.4) to give a 5% (v/v) solution. The RBC suspension was added to HEPES-buffered saline, 1% Triton X-100, and samples and incubated for 60 min at 37 °C. After centrifugation with Heraeus table top centrifuge 5805R at 12,000 rpm at 4 °C, the supernatants were transferred to a 96-well plate. Hemolytic activity was determined by measuring the absorption at 550 nm using benchmark microplate reader (Biorad Microplate reader 5804R). The samples with 0% lysis (HEPES buffer saline) and 100% lysis (1% Triton X-100) were referred as +ve and −ve control respectively. All assays were performed in triplicate. Hemolytic effect of each treatment was expressed as percent cell lysis relative to the untreated control cells (% control) is defined as

$$\text{hemolysis (\%)} = \frac{\text{Abs at 550 samples} - \text{Abs at 550 } - \text{ve control}}{\text{Abs at 550} + \text{ve control} - \text{Abs at 550 } - \text{ve control}} \times 100 \quad (3)$$

2.10.2. Cytotoxicity assay

3T3 cell line was cultured in RPMI-1640 medium with 2 mM L-glutamine which was supplemented with 10% fetal bovine serum (FBS), 100 units/mL penicillin, and 0.1 mg/mL streptomycin. The cells were maintained in T-25 flasks at 37 °C, 5% CO_2 in a humidified incubator with a feeding cycle of 2 days. Confluent cell monolayers were trypsinized (0.25% Trypsin + 0.1% EDTA), centrifuged and were suspended in RPMI in fresh T-25 flasks. Cells were seeded at a density of 3×10^3 cells/cm^2 in RPMI with a feeding cycle of 2 days.

The copolymers were dissolved in sterile water (pH 7.4) and filtered through 0.2 μm polycarbonate filter. Then the samples were diluted to desired concentrations. Cell suspensions were seeded into a 96-well plate at 3×10^3 cells/well in 0.1 mL complete medium. The cells were allowed to adhere and grow for 24 h at 37 °C in an incubator (Heraeus Hera Cell), after which the medium was aspirated and replaced with 0.1 mL fresh medium containing control and samples with the desired concentrations. After 48 h, the culture medium was removed, the cells were washed with sterile phosphate buffer saline (PBS) (0.1 mL/well) three times. Cell viability was assessed using a conventional MTT (3-(4,5-dimethyl-2-thiazolyl)-2,5-diphenyl-2H-tetrazolium bromide) dye reduction assay. 0.1 mL of MTT reagent in PBS (1 g/L) was added to each well. After 4–5 h incubation, the MTT reagent mixture was gently removed. Then 0.1 mL DMSO was added into each well to dissolve the purple formazan precipitate which was reduced from MTT by the viable cells with active mitochondria. The formazan dye was measured spectrophotometrically using benchmark microplate reader at 550 nm. All assays were performed in triplicate. The cytotoxic effect of each treatment was expressed as percent cell viability relative to the untreated control cells (% control) defined as:

$$\text{cell viability (\%)} = \frac{\text{absorbance at 550 of treated cells with samples}}{\text{absorbance at 550 of control cells without samples}} \times 100 \quad (4)$$

2.10.3. Statistical analysis

Statistical analysis was performed using Microcal TM Origin 6.0 (Microcal Software, MA, USA). Comparison of the results between the different materials used one-way analysis of variance (ANOVA). The results were expressed as mean ± SD unless otherwise noted; $^{***}p < 0.001$ was considered statistically significant.

3. Results and discussion

3.1. Molecular characterization

The chemical structures of the copolymers were verified by FT-IR and ^{1}H NMR spectroscopy. The absence of characteristic vinylic peak (1600 cm^{-1}) in the FT-IR spectrum supports the formation of polymeric structure. Similarly, the disappearance of the peaks for the vinylic protons and broadening of proton peaks in the ^{1}H NMR spectrum confirmed polymeric structure. The chemical composition of the copolymers was determined by use of ^{1}H NMR spectrum measured in $CDCl_3$ solvent with traces of CD_3OD. The representative ^{1}H NMR spectra of the acid form of SAPhe-DA(0.16) is presented in Fig. S1 of "Supplementary Materials". The signals at 4.6 and 3.3 ppm correspond, respectively, to the proton bonded to the carbon adjacent to nitrogen (br, ^{1}H, –NH–*CH*–COOH) and to the methylene groups attached to phenyl group (br, 2H, –CH–CH_2–Ph) of the *N*-acryloyl-L-phenylalanine monomer (APhe). The peaks of the *N*-dodecylacrylamide (DA) monomer are observed at 1.2 ppm (br, 18H, –NH–CH_2–CH_2–$(CH_2)_9$–CH_3), and 0.8 ppm (m, 3H, –NH–CH_2–CH_2–$(CH_2)_9$–CH_3). The signals corresponding to the methylene and methine protons on the main chain are observed from 2.0 to 2.5 ppm. The integrated signals at 4.6 ppm for *N*-acryloyl-L-phenylalanin monomer (SAPhe), and 0.8 ppm for DA were employed to calculate the mole fraction of the two monomers in the copolymer. The copolymer composition thus obtained almost matched the feed composition. Similar result was also obtained for the other copolymers employed in this work.

The number-average molecular weights (M_n) of the synthesized copolymers were determined by GPC using polystyrene as standard. The data have been collected in Table 1. For comparison purposes, we have also included the data for SAVal-DA(0.16) copolymer previously reported by us (Dutta et al., 2009a). It can be observed that these HMPs have molecular weight ca. 1/6 or 1/2 of SAVal-DA(0.16). The PDI values of these copolymers are also greater than that of SAVal-DA(0.16) copolymer, indicating wider distribution of molar mass and hence size. Among the HMPs, SALeu-DA(0.16) has the lowest molecular weight and highest PDI value.

Table 1
Weights average (M_w), number average (M_n) molecular weights, and polydispersity index (PDI) of copolymers.

Copolymer	M_w ($\times 10^{-5}$ g/mol)	M_n ($\times 10^{-5}$ g/mol)	PDI
SAGly-DA(0.16)	6.5	4.8	1.34
SAPhe-DA(0.16)	5.3	2.9	1.83
SALeu-DA(0.16)	2.1	0.85	2.47

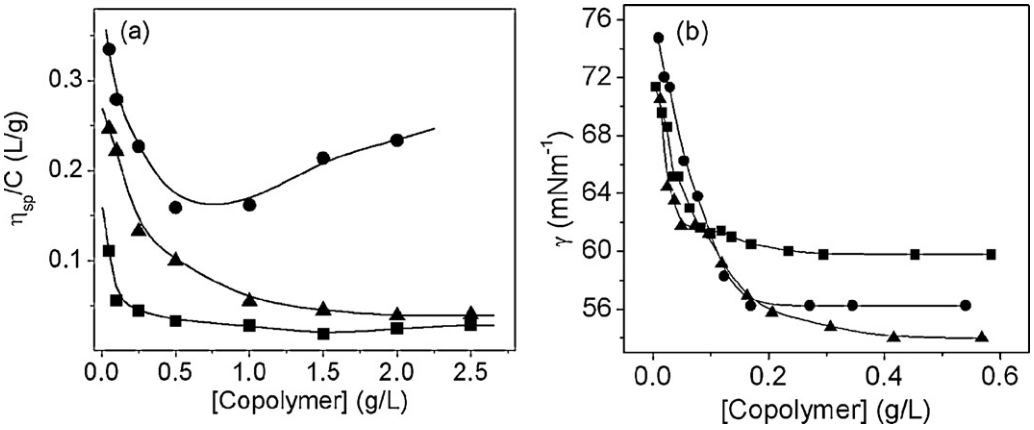

Fig. 1. Plots of (A) η_{sp}/C and (B) γ versus [copolymer] for (■) SAGly-DA(0.16), (●) SALeu-DA(0.16), and (▲) SAPhe-DA(0.16) at 30 °C.

3.2. Solution behavior

For all the three copolymers, the variation of reduced viscosity with [copolymer] is shown by the plots in Fig. 1(A). The polyelectrolyte behavior is clearly evident from the increase of η_{sp}/C with the decrease of polymer concentration. The surface tension (γ) of water upon addition of increasing concentration of polymers was also measured for all the three copolymers. The γ versus [copolymer] plots for the copolymers have been depicted in Fig. 1(B). The surface activity of the HMPs is shown by the decrease of surface tension of water with increasing concentration of the copolymers. Of the HMPs studied, SAPhe-DA(0.16) is most surface-active. The surface activity decreases in the order SAPhe-DA(0.16) > SALeu-DA(0.16) > SAGly-DA(016). This suggests that amphiphilicity of the copolymers increases with the increase in hydrophobicity of the amino acid side chain. Similar observation has also been reported for the *N*-acyl amino acid surfactants (Miyagishi et al., 1989). However, this could also be due to their difference in molecular weight (M_w).

3.3. Nanoparticle formation

Our earlier reports on SAVal-DA(0.16) (Dutta et al., 2009a) suggested formation of nanosize particles in aqueous solution. Therefore, TEM imaging (Fig. 2) of aqueous solutions of the HMPs was performed to investigate size and shape of nanoparticles formed. The micrographs of SAGly-DA(0.16), SAPhe-DA(0.16), and SALeu-DA(0.16) exhibits spheroidal nanoparticles. Although the TEM image of SAPhe-DA(0.16) (micrograph C) is not very good but the formation of smaller aggregates (<50 nm) is still predictable. The diameter of the nanoparticles, formed by the copolymers ranges between 20 nm and 150 nm. However, some smaller particles (<20 nm) are also visible. However, the particles formed by SALeu-DA(0.16) (micrograph B) appear to be agglomerated together forming a big cluster. A close look at the microstructures still suggests that the diameters of the individual aggregates are much smaller than the aggregates of SAGly-DA(0.16). This is probably because of the strong hydrophobic interaction. It is quite obvious that the increased hydrophobicity of the hydrophilic head group enhances the chain packing causing an overall reduction in size of the polymeric aggregates.

3.4. Hydrodynamic size of the nanoparticles

DLS experiments were performed for direct measurement of hydrodynamic radius ($\langle R_h \rangle$) of the nanoparticles formed in aqueous solution of the copolymers. Intensity average size distributions at two different concentrations (0.1 and 1.0 g/L) at a measurement angle of 90° are shown in Fig. 3. As observed, at low concentration, the copolymers SAGly-DA(0.16) and SAPhe-DA(0.16) have monomodal and bimodal distribution with a mean diameter of 120 and 90 nm, respectively. On increasing polymer concentration the distribution for SAGly-DA(0.16) becomes bimodal with a small peak appearing in the lower diameter range. On the other hand, the biomodal peaks of the copolymer SAPhe-DA(0.16), merge into a single one. In contrast, a broad distribution with a mean diameter of 180 nm was observed for copolymer SALeu-DA(0.16) even at very low concentrations. It gets further broadened with increasing polymer concentration. To measure $\langle R_h \rangle$, the diffusion coefficient was also determined at different scattering angle in the range of 40–120° (results not included). The $\langle R_h \rangle$ values corresponding to 0.1 and 1.0 g/L copolymer solutions were calculated

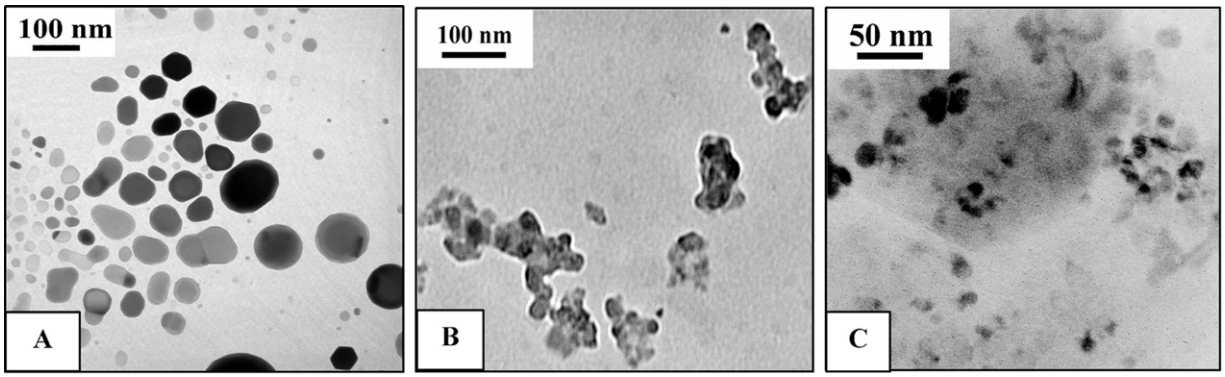

Fig. 2. TEM images of (A) 0.3 g/L SAGly-DA(0.16), (B) 0.1 g/L SALeu-DA(0.16), (C) 0.1 g/L SAPhe-DA(0.16) in pH 8 phosphate buffer.

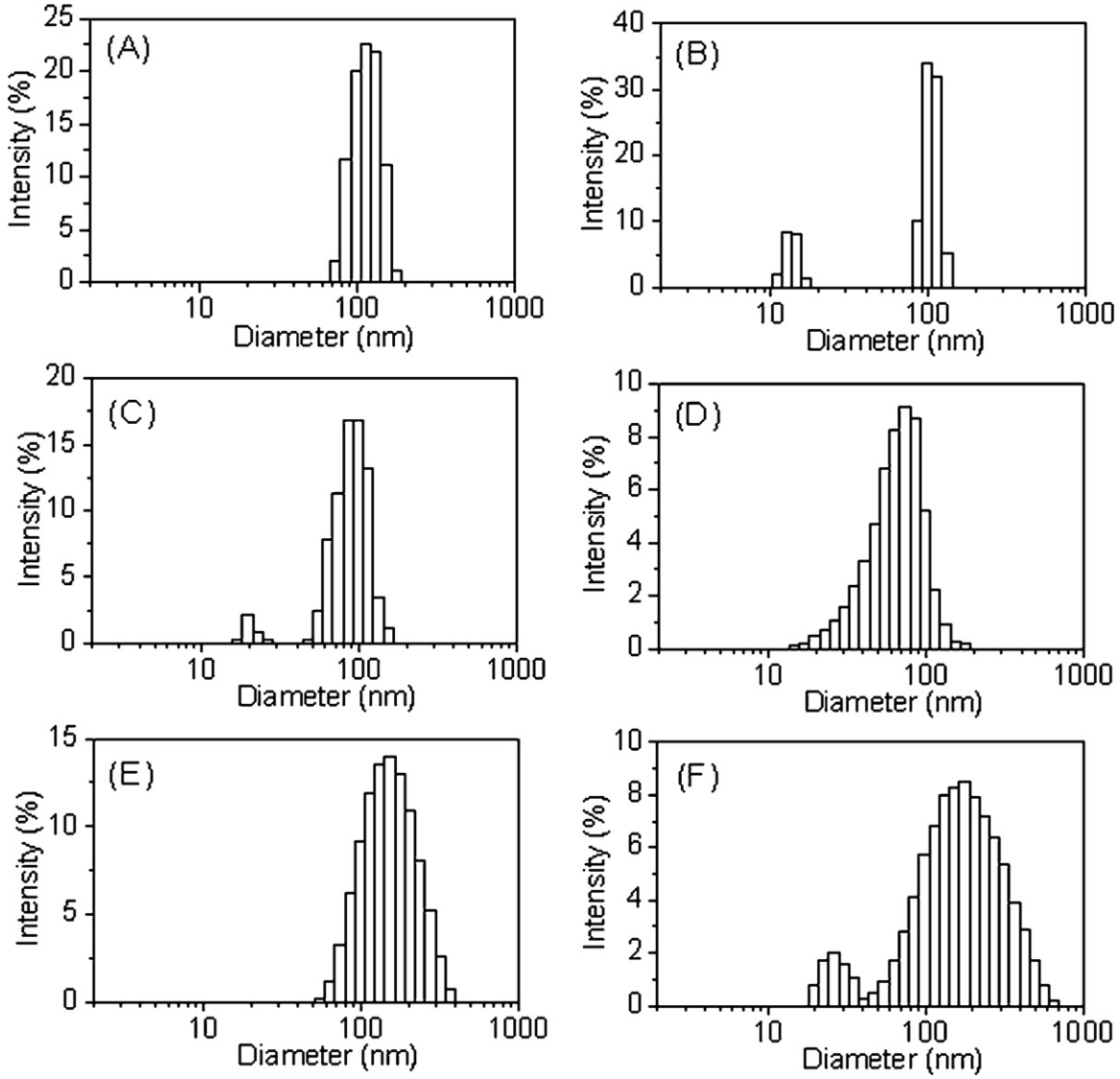

Fig. 3. Size distribution of (A) 0.1 g/L and (B) 1.0 g/L of SAGly-DA(0.16); (C) 0.1 g/L and (D) 1.0 g/L of SAPhe-DA(0.16); (E) 0.1 g/L and (F) 1.0 g/L of SALeu-DA(0.16).

from the values of diffusion constant obtained from the respective Γ–q^2 plots (not shown here) and have been included in Table 2. The concentration dependence of $\langle R_h \rangle$ was also measured for all the three copolymers. As seen in Fig. 4, the values $\langle R_h \rangle$ of the copolymers increase only slightly with increasing polymer concentration. This suggests that the morphology of particles remains almost unchanged with increasing copolymer concentration. Thus the results of DLS measurements along with the results obtained from TEM studies suggest existence of nanosize particles in solutions of higher polymer concentrations.

Table 2
Critical aggregation concentration (*CAC*), polarity parameters ($\Delta\lambda$ and I_1/I_3), microviscosity (η_m), mean hydrodynamic diameter $\langle R_h \rangle$, and zeta potential (ζ) for 1.0 g/L SAGly-DA(0.16), SAPhe-DA(0.16), and SALeu-DA(0.16) in aqueous phosphate buffer solution (pH 8).

Physical properties	SAGly-DA(0.16)	SAPhe-DA(0.16)	SALeu-DA(0.16)
$CAC \times 10^4$ (g/L)	29 ± 5	15 ± 4	4 ± 2
$\Delta\lambda$ (±3 nm)	26	36	42
I_1/I_3 (±0.05)	1.25	1.07	0.96
η_m (mPa s)	65.1	65.9	82.02
$\langle R_h \rangle$ (nm)	53 ± 4	36 ± 6	80 ± 5
ζ (mV)	−10.2	−21.7	−25.2

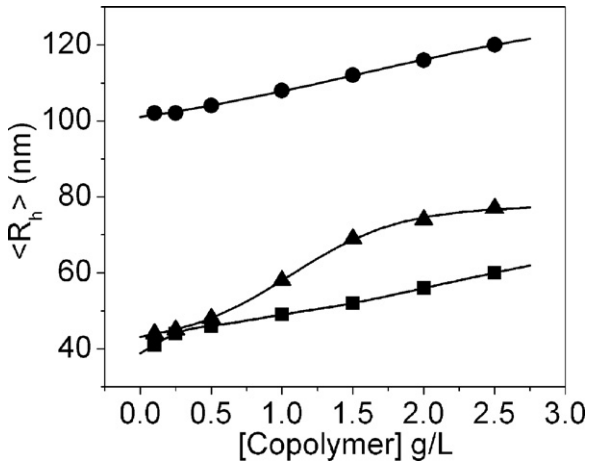

Fig. 4. Plots of average hydrodynamic radii ($\langle R_h \rangle$) versus [copolymer] in pH 8 with 0.1 M NaCl at 25 °C; (■) SAGly-DA(0.16), (●) SALeu-DA(0.16), and (▲) SAPhe-DA(0.16).

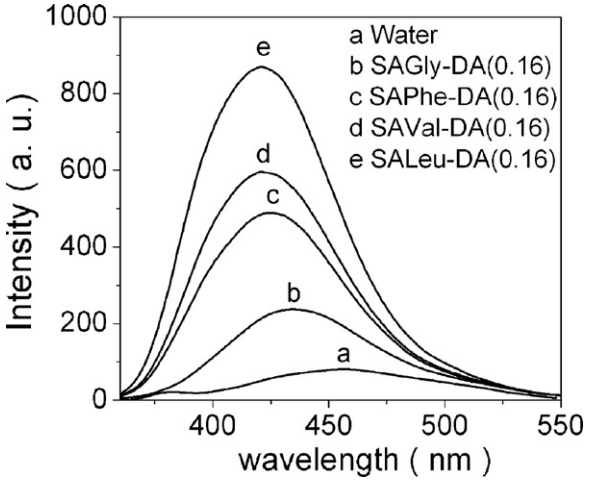

Fig. 5. Fluorescence emission spectra of NPN in water and in the presence of copolymer (0.1 g/L).

3.5. Electrical charge of the nanoparticles

In order to determine the electrical charge of the nanoparticles, we measured zeta-potential (ζ) of the 1 g/L aqueous solutions of each of the three copolymers. The ζ-values are included in Table 2. The relatively lower but negative ζ-values the copolymers suggest that the particles are weakly negatively charged. This is perhaps because the measurements were done in buffered solution. The added Na^+ ions reduce inter-particle ionic repulsion by screening the negative charge and thereby cause agglomeration of the particles as shown by the TEM pictures (Fig. 2). Among the three copolymers, SALeu-DA(0.16) and SAPhe-DA(0.16) have almost equal ζ-value. On the other hand, SAGly-DA(0.16) has the lowest zeta-potential. This difference might be due to either difference in polymer chain length (i.e., molar mass) or due to the difference in ionization behavior of the $-COO^-$ groups in the polymer chain. This could also be linked to the difference in aggregation number (i.e., number of polymer chains per particle) in the case polymer chains associate to form aggregates. This has been studied by fluorescence probe technique as described below.

3.6. Self-assembly studies

Our earlier studies on SAVal-DA(0.16) copolymer suggested self-assembly of the polymer chains even in very dilute aqueous solution forming nanosize aggregates. Therefore, the self-assembly behavior of the copolymers in aqueous solution were investigated by use of NPN as a fluorescent probe. NPN is a well known hydrophobic fluorescent probe which changes its photophysical properties with the change of environment (Mohanty et al., 2007; Khatua et al., 2006; Mohanty and Dey, 2004; Kujawa et al., 2006). For example; it is weakly fluorescent in aqueous medium. However, the fluorescence emission spectrum of NPN undergoes a blue shift accompanied by a huge increase in intensity upon solubilization into the non-polar environment of micelles. The fluorescence emission spectra of NPN taken in aqueous solution (0.1 g/L) of the copolymers are presented in Fig. 5. For comparison purposes, the spectrum in the presence of SAVal-DA(0.16) copolymer has also been included. As seen, the emission maxima underwent a blue shift with a simultaneous rise in emission intensity in the presence of copolymers, suggesting formation of hydrophobic domains. The blue shift, $\Delta\lambda$ (= λ_{max} (water) − λ_{max} (sample)), relative to the emission spectrum in water was recorded for all the HMPs and the data are included in Table 2. The maximum blue shift is observed with SALeu-DA(0.16) copolymer with highest hydrophobicity of the amino acid side chain. The amino acid head group of SAGly-DA(0.16) being more hydrophilic has the lowest $\Delta\lambda$ value. This suggests that the NPN probe is solubilized near the amino acid head group region. In fact, similar observation has also been reported for micelles of surfactant monomers (Roy and Dey, 2005; Mohanty and Dey, 2007). The results also suggest that the degree of water penetration is decreased with the increase in the number of carbon atoms in the chain attached to the pendant amino acid hydrophilic head group of the copolymers.

It is important to note that the emission intensity at the λ_{max} of NPN fluorescence (Fig. 5) increases in the order water < SAGly-DA(0.16) < SAPhe-DA(0.16) < SAVal-DA(0.16) < SALeu-DA(0.16). This can be attributed to the increasing solubility of NPN probe in the copolymer aggregates, which increases with the increase of hydrophobicity of the amino acid side chain. The variation of the relative fluorescence intensity (I/I_o) and blue shift, $\Delta\lambda$ of NPN probe with the copolymer concentration have further been shown in Fig. 6. The plots show a rise in I/I_o as well as $\Delta\lambda$ values with increasing [copolymer]. Also these HMPs exhibit a concentration-independent region in the respective plots suggesting hydrophobic domain formation through inter-chain association above a critical concentration, called critical aggregation concentration (CAC). The chain association occurs through the van der Waals interaction and hydrophobic effect of the hydrophobe units in the polymer chain. The *CAC* values as obtained from the inflection point of the plots have been listed in Table 2. It is observed that even

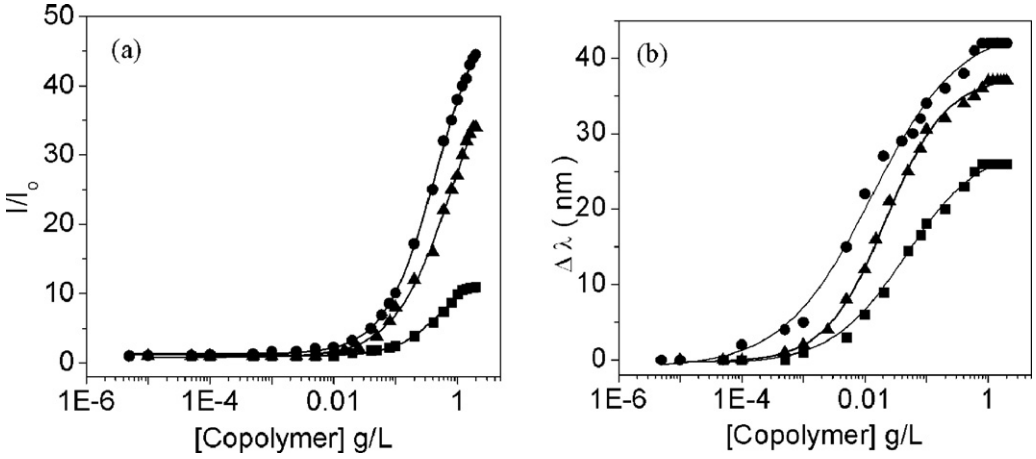

Fig. 6. Plots of (A) relative fluorescence intensity (I/I_o) and (B) $\Delta\lambda$ of NPN probe versus [copolymer] at 30 °C; (■) SAGly-DA(0.16), (●) SALeu-DA(0.16), and (▲) SAPhe-DA(0.16).

Table 3
Solubility (mg/L), solubilization capacity (mg/g), and encapsulation efficiency (%) of griseofulvin for 1.0 g/L copolymer solution at pH 7.4.

Copolymer	Solubility (mg/L)	Solubilization capacity, S_{cp} (mg/g)	Encapsulation efficiency, E_{ef} (%)
SAGly-DA(0.16)	22.1 ± 1.1	12.1 ± 1.1	12.1
SALeu-DA(0.16)	39.3 ± 3.1	29.3 ± 3.1	29.3
SAPhe-DA(0.16)	32.3 ± 2.6	22.4 ± 2.6	22.4

though SAGly-DA(0.16) has highest molecular weight, its *CAC* value is greater than those of the other L-amino acid containing HMPs, suggesting an influence of hydrophobicity of the amino acid head group. Higher value of *CAC* for SAGly-DA(0.16) is due to the hydrophilic nature of glycine. In fact, such an observation has also been reported for sodium salts of different *N*-acyl amino acids by Miyagishi and co workers (Miyagishi et al., 1989). Among the chiral amino acid containing copolymers, SALeu-DA(0.16) has the lowest *CAC* value which is consistent with the higher hydrophobicity of the side chain of L-leucine. The data in Table 2 suggest that an additional $-CH_2-$ unit in the amino acid side chain reduces the *CAC* to 3.75×10^{-4} g/L which is ~1.8 times lower than that of SAVal-DA(0.16) (9×10^{-4} g/L).

The micropolarity of the hydrophobic domains formed by the copolymers in aqueous solution was further determined at two different concentrations (0.1 and 1.0 g/L) above *CAC* by measuring the I_1/I_3 ratio of the pyrene probe, which is normally solubilized in the hydrocarbon core of surfactant micelles (Kalyanasundaram and Thomas, 1977). The data are presented in Table 2. The I_1/I_3 values for all the copolymers are much lower compared to that in bulk water. This suggests that the microenvironment of the pyrene probe is non-polar like hydrocarbon solvents and is consistent with the results obtained using NPN probe. In comparison to SAPhe-DA(0.16) and SALeu-DA(0.16) copolymers, the microenvironment of the aggregates of SAGly-DA(0.16) is more polar. Relatively higher polarity of the microenvironment of the aggregates of SAGly-DA(0.16) is due to much polar head group which allows more water molecules to penetrate into the hydrocarbon core of the aggregates.

3.7. Microviscosity

To get additional information about the microenvironments of the copolymer aggregates microviscosity (η_m) was determined in aqueous solution containing 1.0 g/L copolymer. The η_m values of the copolymer aggregates were obtained from steady-state fluorescence anisotropy (r) and fluorescence lifetime (τ_f) data of the DPH probe. The time-resolved fluorescence data have been summarized in Table S1 of "Supplementary Materials". The η_m values were calculated from the SED and Perrin's equations (Lakowicz, 1983) using average lifetime of the fluorescence decay (for details see Supplementary Materials). For all the HMPs, the η_m value is large compared to that of micelles of ionic surfactants, such as SDS (16.33 mPa s) (Roy et al., 2005). This is because the hydrophobes are covalently linked with the polymer backbone and hence are less flexible. It is observed that the microdomains of the copolymer SAGly-DA(0.16) has η_m value almost equal to that of SAPhe-DA(0.16). On the other hand, SALeu-DA(0.16) has the highest η_m value. The data in Table 3 suggest that the η_m value of the copolymer micelles increases with increasing size of the amino acid side chain that increases rigidity of the hydrophobic domains.

3.8. Solubilization of griseofulvin

The results of the self-assembly studies discussed above indicate that the microenvironment of the copolymer micelles are sufficiently hydrophobic and can act as a microreservoir for poorly water-soluble pharmaceutically active agents. Therefore, to gain preliminary knowledge on the ability of the present amino acid based HMPs in incorporating poorly water-soluble drug molecules into their inner hydrophobic core we have selected a model drug GF, which is an antifungal drug and widely used for the treatment of skin disease (Bennett et al., 2000). Although it has strong antifungal activity, the poor aqueous solubility (10 mg/L at 25 °C) sometimes limits its clinical application. Various formulations like solid dispersions, liposomes, bio-adhesive polymers have therefore been reported earlier to improve its solubility (Chiou and Riegelman, 1971; Sue et al., 1993; Tur et al., 1997). We have earlier shown that aqueous solubility of GF is increased 4 times in the presence of SAVal-DA(0.16) copolymer (Dutta et al., 2009b). Since, as discussed later, all three HMPs exhibited negligible toxicity up to 1.0 g/L concentration, we preferred to investigate the solubility of GF at 1 g/L copolymer concentration. Equilibrium solubility, solubilization capacity (S_{cp}), solubilization efficiency (S_{ef}) (described in the experimental section) estimated for the drugs under the physiological condition (pH 7.4, 37 °C) are summarized in Table 3. As seen, among the three copolymers, SALeu-DA(0.16) with strong internal hydrophobicity as reflected by I_1/I_3 and η_m values can upload 39.3 mg/g of HMP with encapsulation efficiency of 29.3% which is 2.4 and 1.3 times higher than that of SAGly-DA(0.16) and SAPhe-DA(0.16) copolymers, respectively. It is worth mentioning here, the solubility of GF determined in presence of these newly synthesized high-molecular-weight HMPs are far higher than the previously reported micelle-forming neutral surfactants, e.g., Tween 80 (3.4 mg/g), and Creomphor EL (2.6 mg/g) (Balakrishnan et al., 2004) and triblock copolymers (M_n ~ 5000–7000 g/mol) of ethylene oxide and phenylglycidyl ether (ca. 4.0–17.8 mg/g) (Taboada et al., 2005).

3.9. Thermal stability of nanoparticles

The thermal stability of the copolymer micelles was investigated by fluorescence probe technique using DPH probes. The fluorescence anisotropy of DPH was measured in aqueous buffer solution (pH 7.4) in the presence of 0.25 g/L copolymers at various temperatures. The plots of steady-state fluorescence anisotropy (r) of DPH as a function of temperature in solution containing 0.25 g/L copolymer are presented in Fig. 7. The decrease of r-value suggests that as the temperature is increased the microenvironments of the aggregates become less viscous. It is important to note that despite lower molecular weight, the change in r-value at higher temperatures

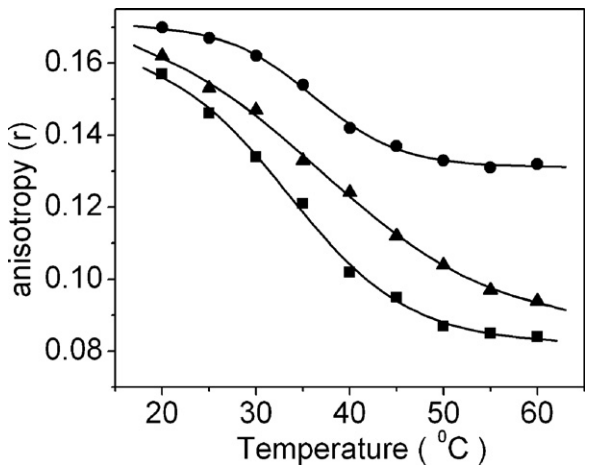

Fig. 7. Plots of fluorescence anisotropy (r) of DPH at different temperatures for 0.25 g/L (■) SAGly-DA(0.16), (●) SALeu-DA(0.16), and (▲) SAPhe-DA(0.16).

Table 4
pK_a values of the copolymers and chain melting temperature (T_m) of the aggregates in aqueous medium at 30 °C; $\langle R_h \rangle$ values of the aggregates of the copolymers SAGly-DA(0.16), SAPhe-DA(0.16), and SALeu-DA(0.16) at different temperatures in pH 8.

Copolymer	pK_a	T_m (°C) (±0.5)	Concentration (g/L)	$\langle R_h \rangle$ (±6 nm)		
				25 °C	40 °C	55 °C
SAGly-DA(0.16)	5.5	33.4	0.25	44	115.5	142
			2.0	56	78	79
SAPhe-DA(0.16)	6.6	36.7	0.25	45	72	80.5
			2.0	74	75.5	77.5
SALeu-DA(0.16)	6.7	36.0	0.25	102	106	107
			2.0	116	118	117

is relatively less for the nano-aggregates of SALeu-DA(0.16), indicating that *r*-value is less sensitive to temperature as the probe molecule is solubilized in the core of the compact hydrophobic domains. The melting temperatures of the copolymer aggregates were determined from the inflection point of the respective titration curve. The data are listed in Table 4. Most of the HMPs have T_m value ca. 37 °C. However, SALeu-DA(0.16) has slightly lower T_m value. This means that the nano-aggregates of SALeu-DA(0.16) have higher thermal stability as compared to those of SAPhe-DA(0.16) and SAGly-DA(0.16). The results suggest that the nano-aggregates of all these HMPs can be employed for temperature-induced drug release.

In aid to the results of fluorescence probe studies, thermal stability of the copolymer micelles were also examined for both dilute and concentrated solutions of the all the copolymers employing DLS technique. Table 4 compares the change in $\langle R_h \rangle$ value of the copolymers, SAGly-DA(0.16), SAPhe-DA(0.16), and SALeu-DA(0.16) at three different temperatures. As observed, at low concentration, the copolymer SAGly-DA(0.16) has $\langle R_h \rangle$ = 44 nm at 25 °C. Bringing the solution temperature at 40 °C the $\langle R_h \rangle$ value increases to 115.5 nm which on further heating to 55 °C the value raises to 142 nm. The similar trend was also observed for the copolymer, SAPhe-DA(0.16). Thus, the $\langle R_h \rangle$ increases from 45 nm to 80.5 nm upon heating the polymer solution from 25 °C to 40 °C. However, the increase was relatively less between 40 and 55 °C. Unlike copolymers, SAGly-DA(0.16) and SAPhe-DA(0.16), the $\langle R_h \rangle$ for SALeu-DA(0.16) remained almost unchanged in the same temperature range. Again at high concentration (2 g/L), while the copolymer SAPhe-DA(0.16) and SALeu-DA(0.16) did not exhibit any response to temperature, the small change in $\langle R_h \rangle$ was observed for the copolymer SAGly-DA(0.16) between 40 and 50 °C, which remained constant thereafter. From the results of fluorescence and DLS measurements it is quite evident that the amino acid head group has a strong influence on the stability of the micellar aggregates of the copolymers.

3.10. pH-triggered release of NPN

In order to investigate drug release as a result of pH change, we employed NPN as a probe molecule. Fig. 8 shows the variation of $\Delta\lambda$ of NPN probe as a function solution pH. As observed, in going from higher to lower pH the $\Delta\lambda$ value steadily increases for SAGly-DA(0.16), and SAPhe-DA(0.16) copolymers. However, a very little change in $\Delta\lambda$ was observed for SALeu-DA(0.16) in the same pH regime. Therefore, on decreasing the pH while the copolymer SAGly-DA(0.16), and SAPhe-DA(0.16) are undergoing an open to closed structural transition, no such structural transition was observed for SALeu-DA(0.16) copolymer. Since the copolymer SALeu-DA(0.16) at 0.25 g/L polymer concentration is already existing as compact structure resulting from the enhanced chain packing of the hydrophobe as well as hydrophobic side chain of the amino acid head group, the probe molecules are solubilized deep into the hydrocarbon core so that the protonation of the carboxylate groups does not affect the overall conformation of the copolymer. However, because of the relatively less polar head group, the copolymers, SAGly-DA(0.16) and SAPhe-DA(0.16) at higher pH (~8) have weaker hydrophobic interaction among the long hydrocarbon chains and remained in a less dense state. As a result of the decrease in solution pH, the $-COO^-$ groups become progressively neutralized, which in turn favor the chain packing. Consequently, the probe molecules that remained in bulk water get partitioned into the more compact hydrophobic domains. The pK_a value of the copolymers SAGly-DA(0.16), SALeu-DA(0.16), and SAPhe-DA(0.16) as obtained from the corresponding plot in Fig. 8 are included in Table 4. SALeu-DA(0.16) and SAPhe-DA(0.16) have highest pK_a values ca 6.6 and 6.7, respectively and SAGly-DA(0.16) has the lowest pK_a values (5.5). This is consistent with their molecular weight. However, effect of the amino acid side chain cannot be ruled out.

3.11. Biocompatibility studies

3.11.1. Hemocompatibility

Hemolytic assays were performed to investigate about the compatibility of these new copolymers with RBC membranes. % Hemolysis of RBCs against 0.1 and 1.0 g/L copolymers are compared with the +ve (1% triton X-100) and −ve control (Hepes buffer saline) in Fig. 9(A). It is seen that at dilute copolymer concentration all three copolymers have negligible hemolysis (<3%) as compared to +ve control. As the concentration increases to 1.0 g/L the % hemolysis slightly increases to 2.7 ± 0.21, 3.9 ± 0.15, and 3.7 ± 0.11% respectively for SAGly-DA(0.16), SAPhe-DA(0.16), and SALeu-DA(0.16) copolymers. It is interesting to see that the % hemolysis at higher concentration is quite similar to our earlier reported copolymer SAVal-DA(0.16) (3.5 ± 0.13%) (Dutta et al., 2011). In general, hemolysis depends on the hydrophilic/hydrophobic balance of

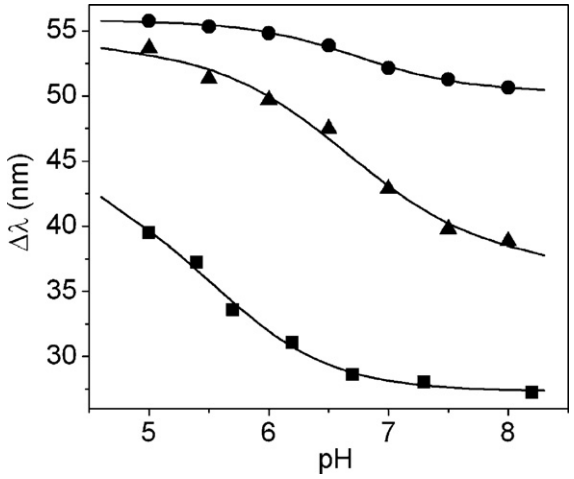

Fig. 8. Plot of shift of emission maximum ($\Delta\lambda$) of NPN at different solution pH of 0.25 g/L copolymer; (■) SAGly-DA(0.16), (▲) SAPhe-DA(0.16), and (●) SALeu-DA(0.16).

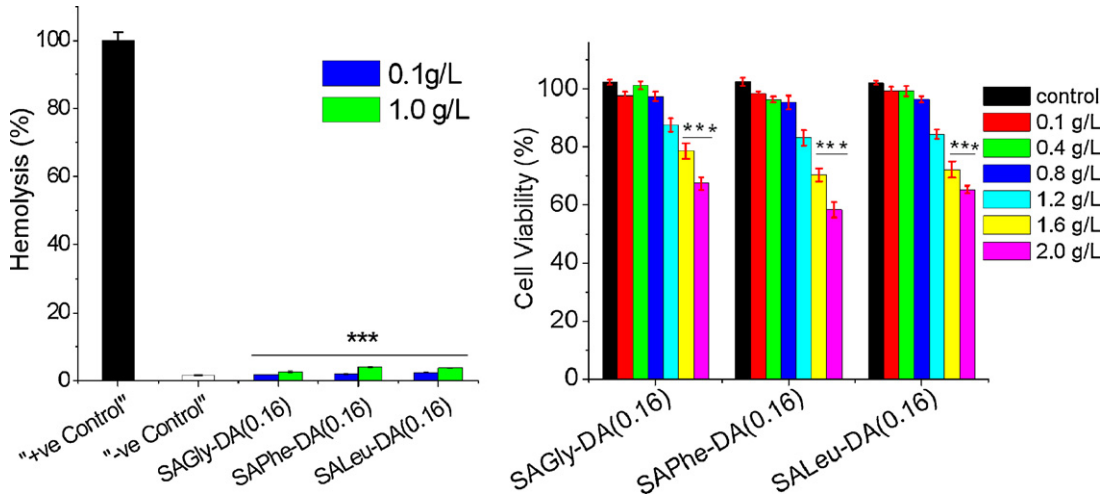

Fig. 9. (A) Percentage of hemolysis of copolymers at 0.1 g/L and 1 g/L concentration at physiological pH (7.4). (B) MTT assay based fibroblast cell line 3T3 cell viability (in %) as a function of concentration for copolymers at physiological pH (7.4). Significant difference is shown as $^{***}p < 0.001$ versus +ve control. The bars indicate the means ± SD ($n = 3$).

the amphiphilic polymers and it is often found that amphiphilic polymers with either longer alkyl chain or greater degree of hydrophobic substitution causes higher cell lysis by insertion of hydrophobic counterpart followed by charge species into the red blood cell membrane (Kuroda et al., 2009; Venkataraman et al., 2010). In our investigations, the copolymers have the identical degree of hydrophobic substitution with similar alkyl chain length but they differ in the hydrophobicity of hydrophilic head group. Therefore, considering the overall hydrophobicity it can be anticipated that all these copolymers will contribute to the similar hemolytic behavior which is consistent with the finding results in the present investigation. Above all, since the % hemolysis is less than 5% in all the cases, they can be regarded as non-hemolytic and can be further considered for exploring their uses in intravenous drug delivery applications.

3.11.2. Cytotoxicity

In order to investigate the effects of the copolymers on cell proliferation and cytotoxicity, we conducted in vitro MTT (3-(4,5-dimethylthiazol-2-yl)-2,5-diphenyltetrazolium bromide) dye reduction assays on mammalian 3T3 cell line in the concentration range of 0.1–2.0 g/L at physiological pH (7.4) similar to the method reported earlier by our group. Fig. 9(B) presents the cell viability (%) as a function of polymer concentration. As shown, at a concentration lower than 1.2 g/L, all three copolymer showed lower cytotoxicity against 3T3 cells and cell viabilities are more than 80% which is very promising result as far as the drug delivery is concern. As the concentration increases beyond 1.2 g/L toxicity increase as a result of high negative charge density from the amino acid counterpart which is rather expected phenomena in cell proliferation assay. However, it is quite interesting to observe that like hemolytic behavior, the hydrophobicity of the amino acid head group has also a very little influence on the cell proliferation and thus showing very similar kind of cell viability against the 3T3 cell line.

4. Conclusions

In summary, we have described in detail the syntheses, physicochemical characterization, and biocompatibility evaluation of three new amino acids based hydrophobically modified polyelectrolytes (HMPs) with glycine, L-valine, and L-phenylalanine as amino acid constituent in the hydrophilic head group. These HMPs are amphiphilic in nature and are surface-active. As characterized by the fluorescence probe studies, all three copolymers self-assemble in aqueous buffered solution above *CAC* providing non-polar hydrophobic microdomains. Among the three copolymers, SALeu-DA(0.16) with longer amino acid side chain has the least *CAC* value followed by SAPhe-DA(0.16) and SAGly-DA(0.16), indicating that the longer amino acid side chain has a stronger tendency to associate in self-assembling process. TEM results indicate that these copolymers self-assemble to form micelles like structures having diameters in the range from 20 nm to 150 nm. SALeu-DA(0.16) copolymer with strong hydrophobic interaction however found to have smaller diameter with agglomerated micellar morphology. The pK_a and melting temperature (T_m) of these copolymers are in the range of 5.5–6.7 and 35–37 °C, respectively which are very close to the physiological systems of human body. As examined by in vitro hemocompatibility these copolymers were found to be biocompatible. In addition, up to a moderate concentration (<1.2 g/L), these HMPs exhibit minimal cytotoxicity against mammalian cell line. They also come out with better solubilizer for poorly water-soluble antifungal drug griseofulvin than previously reported low-molecular-weight surfactants which reveal their potential application as drug delivery systems. Further studies on the drug encapsulation and release of other poorly water-soluble pharmaceutically active agents as well as the cell proliferation assays on different human cell lines are presently under investigation and will be presented in a subsequent paper.

Acknowledgements

The authors gratefully acknowledge Department of Science and Technology (DST), New Delhi for financial support (Grant No. SR/S1/PC-68/2008) of this work. PD thanks CSIR (09/081(0519)/2005-EMR-I) for a research fellowship. We thank Dr. M. Mandal, SMST, IIT Kharagpur for help with the biological evaluations.

Appendix A. Supplementary data

Supplementary data associated with this article can be found, in the online version, at doi:10.1016/j.ijpharm.2011.10.011.

References

Aumelas, A., Serrero, A., Durand, A., Dellacherie, E., Leonard, M., 2007. Nanoparticles of hydrophobically modified dextrans as potential drug carrier systems. Colloid Surf. B: Biointerfaces 59, 74–80.

Balakrishnan, A., Rege, B.D., Amidon, G.L., Polli, J.E., 2004. Surfactant-mediated dissolution: contributions of solubility enhancement and relatively low micelle diffusivity. J. Pharm. Sci. 93, 2064–2075.

Bennett, M.L., Fleischer, A.B., Loveless, J.W., Feldman, S.R., 2000. Oral griseofulvin remains the treatment of choice for tinea capitis in children. Pediatr. Dermatol. 17, 304–309.

Brown, M.D., Gray, A.I., Tetley, L., Santovena, A., Rene, J., Schatzlein, A.G., Uchegbu, I.F., 2003. In vitro and in vivo gene transfer with poly(amino acid) vesicles. J. Control. Release 93, 193–211.

Casolaro, M., Bottari, S., Cappelli, A., Mendichi, R., Ito, Y., 2004. Vinyl polymers based on L-histidine residues. Part 1. The thermodynamics of poly(ampholyte)s in the free and in the cross-linked gel form. Biomacromolecules 5, 1325–1332.

Casolaro, M., Bottari, S., Ito, Y., 2006. Vinyl polymers based on L-histidine residues. Part 2. Swelling and electric behavior of smart poly(ampholyte) hydrogels for biomedical applications. Biomacromolecules 7, 1439–1448.

Chiou, W.L., Riegelman, S., 1971. Absorption characteristics of solid dispersed and micronized griseofulvin in man. J. Pharm. Sci. 60, 1376–1380.

Chiu, Y.L., Ho, Y.C., Chen, Y.M., Peng, S.F., Ke, C.J., Chen, K.J., Mi, F.L., Sung, H.W., 2010. The characteristics, cellular uptake and intracellular trafficking of nanoparticles made of hydrophobically-modified chitosan. J. Control. Release 146, 152–159.

Delgado, A.D.S., Leonard, M., Dellacherie, E., 2001. Surface properties of polystyrene nanoparticles coated with dextrans and dextran–PEO copolymers. Effect of polymer architecture on protein adsorption. Langmuir 17, 4386–4391.

Durand, A., Marie, E., Rotureau, E., Leonard, M., Dellacherie, E., 2004. Amphiphilic polysaccharides: useful tools for the preparation of nanoparticles with controlled surface characteristics. Langmuir 20, 6956–6963.

Dutta, P., Dey, J., Ghosh, G., Nayak, R.R., 2009a. Self-association and microenvironment of random amphiphilic copolymers of sodium *N*-acryloyl-L-valinate and *N*-dodecylacrylamide in aqueous solution. Polymer 50, 1516–1525.

Dutta, P., Shrivastava, S., Dey, J., 2009b. Amphiphilic polymer nanoparticles: characterization and assessment as new drug carrier. Macromol. Biosci. 9, 1116–1126.

Dutta, P., Dey, J., Perumal, V., Mondal, M., 2011. Amphiphilic copolymer micelles as carriers of non-steroidal anti-inflammatory drugs: solubilization. In vitro release and biological evaluation. Int. J. Pharm. 407, 207–216.

Guo, Y., Li, M., Mylonakis, A., Han, J., MacDiarmid, A.G., Chen, X., Lelkes, P.I., Wei, Y., 2007. Electroactive oligoaniline-containing self-assembled monolayers for tissue engineering applications. Biomacromolecules 8, 3025–3034.

Hirakura, T., Nomura, Y., Aoyama, Y., Akiyoshi, K., 2004. Photoresponsive nanogels formed by the self-assembly of spiropyrane-bearing pullulan that act as artificial molecular chaperones. Biomacromolecules 5, 1804–1809.

Kalyanasundaram, K., Thomas, J.K., 1977. Environmental effects on vibronic band intensities in pyrene monomer fluorescence and their application in studies of micellar systems. J. Am. Chem. Soc. 99, 2039–2044.

Katanasaka, Y., Ida, T., Asai, T., Shimizu, K., Koizumi, F., Maeda, N., Baba, N., Oku, N., 2008. Antiangiogenic cancer therapy using tumor vasculature-targeted liposomes encapsulating 3-(3,5-dimethyl-1H-pyrrol-2-ylmethylene)-1,3-dihydroindol-2-one, SU541. Cancer Lett. 270, 260–268.

Kawata, T., Hashidzume, A., Sato, T., 2007. Micellar structure of amphiphilic statistical copolymers bearing dodecyl hydrophobes in aqueous media. Macromolecules 40, 1174–1180.

Kedar, U., Phutane, P., Shidhaye, S., Kadam, V., 2010. Advances in polymeric micelles for drug delivery and tumor targeting. Nanomed.: Nanotechnol. Biol. Med. 6, 714–729.

Khatua, D., Gupta, A., Dey, J., 2006. Characterization of micelle formation of dodecyldimethyl-*N*-2-phenoxyethylammonium bromide in aqueous solution. J. Colloid Interface Sci. 298, 451–456.

Kim, J.Y., Choi, W.I., Kim, Y.H., Tae, G., Lee, S.Y., Kim, K., Kwon, I.C., 2010. In-vivo tumor targeting of pluronic-based nano-carriers. J. Control. Release 147, 109–117.

Kim, Y.H., Gihm, S.H., Park, C.R., Lee, K.Y., Kim, T.W., Kwon, I.C., Chung, H., Jeong, S.Y., 2001. Structural characteristics of size-controlled self-aggregates of deoxycholic acid-modified chitosan and their application as a DNA delivery carrier. Bioconjugate Chem. 12, 932–938.

Kujawa, P., Tanaka, F., Winnik, F.M., 2006. Temperature-dependent properties of telechelic hydrophobically modified poly(*N*-isopropylacrylamides) in water: evidence from light scattering and fluorescence spectroscopy for the formation of stable mesoglobules at elevated temperatures. Macromolecule 39, 3048–3055.

Kuroda, K., Caputo, G.A., Degrado, W.F., 2009. The role of hydrophobicity in the antimicrobial and haemolytic activities of polymethacrylate derivatives. Chem. Eur. J. 15, 1123–1133.

Kuroyanagi, Y., Koganei, Y., Shioya, N., 1987. Nessho 13, 206.

Kuroyanagi, Y., Aoki, N., Nakakita, N., Ishihara, S., Chang, C.H., Shioya, N., 1990. Nessho 16, 59.

Lakowicz, J.R., 1983. Principles of Fluorescence Spectroscopy. Plenum Press, New York, p. 132.

Lee, J.Y., Choo, J.E., Choi, Y.S., Park, J.B., Min, D.S., Lee, S.J., Rhyu, H.K., Jo, I.H., Chung, C.P., Park, Y.J., 2007. Assembly of collagen-binding peptide with collagen as a bioactive scaffold for osteogenesis in vitro and in vivo. Biomaterials 28, 4257–4267.

Li, Y., Xiao, K., Luo, J., Lee, J., Pan, S., Lam, K.S., 2010. A novel size-tunable nanocarrier system for targeted anticancer drug delivery. J. Control. Release 144, 314–332.

Miyagishi, S., Asakawa, T., Nishida, M., 1989. Hydrophobicity and surface activities of sodium salts of *N*-dodecanoyl amino acids. J. Colloid Interface Sci. 131, 68–73.

Mohanty, A., Dey, J., 2004. Spontaneous formation of vesicles and chiral self-assemblies of sodium *N*-(4-dodecyloxybenzoyl)-L-valinate in water. Langmuir 20, 8452–8459.

Mohanty, A., Dey, J., 2007. Effect of the headgroup structure on the aggregation behavior and stability of self-assemblies of sodium *N*-[4-(n-dodecyloxy)benzoyl]-L-aminoacidates in water. Langmuir 23, 1033–1040.

Mohanty, A., Patra, T., Dey, J., 2007. Salt-induced vesicle to micelle transition in aqueous solution of sodium N-(4-n-octyloxybenzoyl)-L-valinate. J. Phys. Chem. B 111, 7155–7159.

Mori, H., Sutoh, K., Endo, T., 2005. Controlled radical polymerization of an acrylamide containing L-phenylalanine moiety via RAFT. Macromolecules 38, 9055–9065.

Morishima, Y., 1994. Unimolecular micelles of hydrophobically modified polysulfonates: potential utility for novel photochemical systems. Trends Polym. Sci. 2, 31–36.

Murata, H., Sanda, F., Endo, T., 1996. Highly radical-polymerizable methacrylamide having dipeptide structure. Synthesis and radical polymerization of *N*-methacryloyl-L-leucyl-L-alanine methyl ester. Macromolecules 29, 5535–5538.

Noda, T., Morishima, Y., 1999. Hydrophobic association of random copolymers of sodium 2-(acrylamido)-2-methylpropanesulfonate and dodecyl methacrylate in water as studied by fluorescence and dynamic light scattering. Macromolecules 32, 4631–4640.

Otsuka, H., Nagasaki, Y., Kataoka, K., 2003. PEGylated nanoparticles for biological and pharmaceutical applications. Adv. Drug Delivery Rev. 55, 403–419.

Pilkington-Miksa, M.A., Writer, M.J., Sarkar, S., Meng, Q.H., Barker, S.E., Shamlou, P.A., Hailes, H.C., Hart, S.L., Tabor, A.B., 2007. Targeting lipopolyplexes using bifunctional peptides incorporating hydrophobic spacer amino acids: synthesis, transfection, and biophysical studies. Bioconjugate Chem. 18, 1800–1810.

Ravi Kumar, M.N.V., Muzzarelli, R.A.A., Muzzarelli, C., Sashiwa, H., Domb, A.J., 2004. Chitosan chemistry and pharmaceutical perspectives. Chem. Rev. 104, 6017–6084.

Roy, S., Dey, J., 2005. Effect of hydrogen-bonding interactions on the self-assembly formation of sodium N-(11-acrylamidoundecanoyl)-L-serinate, L-asparaginate, and L-glutaminate in aqueous solution. J. Colloid Interface Sci. 307, 229–234.

Roy, S., Mohanty, A., Dey, J., 2005. Microviscosity of bilayer membranes of some N-acylamino acid surfactants determined by fluorescence probe method. Chem. Phys. Lett. 414, 23–27.

Sabelli, H.C., 1991. Rapid treatment of depression with selegiline-phenylalanine combination. J. Clin. Psychiatry 52, 137.

Sallustio, S., Galantini, L., Gente, G., Masci, G., Mesa, C.L., 2004. Hydrophobically modified pullulans: characterization and physicochemical properties. J. Phys. Chem. B 108, 18876–18883.

Sue, M.S., Liu, K.M., Yu, H.S., 1993. The gastro-intestinal absorption of griseofulvin can be enhanced by encapsulation into liposomes. Yi Xue Ke Xue Za Zhi Gaoxiong (Medline) 9, 1–8.

Taboada, P., Velasquez, G., Barbosa, S., Castelletto, V., Nixon, S.K., Yang, Z., Heatley, F., Hamley, I.W., Ashford, M., Mosquera, V., Attwood, D., Booth, C., 2005. Block copolymers of ethylene oxide and phenyl glycidyl ether: micellization, gelation, and drug solubilization. Langmuir 21, 5263–5271.

Tur, K.M., Ch'ng, H.S., Baie, S., 1997. Use of bioadhesive polymer to improve the bioavailability of griseofulvin. Int. J. Pharm. 148, 63.

Venkataraman, S., Zhang, Y., Liu, L., Yang, Y.Y., 2010. Design, syntheses and evaluation of hemocompatible pegylated-antimicrobial polymers with well-controlled molecular structures. Biomaterials 31, 1751–1756.

Yamamoto, H., Mizusaki, M., Yoda, K., Morishima, Y., 1998. Fluorescence studies of hydrophobic association of random copolymers of sodium 2-(acrylamido)-2-methylpropanesulfonate and *N*-dodecylmethacrylamide in water. Macromolecules 31, 3588–3594.

Yamamoto, H., Morishima, Y., 1999. Effect of hydrophobe content on intra- and interpolymer self-associations of hydrophobically modified poly(sodium 2-(acrylamido)-2-methylpropanesulfonate) in water. Macromolecules 32, 7469–7475.

York, A.W., Kirkland, S.E., McCormick, C.L., 2008. Advances in the synthesis of amphiphilic block copolymers via RAFT polymerization: stimuli-responsive drug and gene delivery. Adv. Drug Delivery Rev. 60, 1018–1036.

Yu, L.M.Y., Kazazian, K., Shoichet, M.S., 2007. Peptide surface modification of methacrylamide chitosan for neural tissue engineering applications. J. Biomed. Mater. Res. Part A 82, 243–255.